Available free online at www.medjchem.com

Mediterranean Journal of Chemistry

Mediterranean Journal of Chemistry **2019**, 8(2), 213-219

High dielectric constant of (1-x)($Na_{0.5}Bi_{0.5}$)TiO_3-x$BaTiO_3$ prepared by the hydrothermal method

Mohmmed Mesrar [1,*], Tajdine Lamcharfi [1], Nor-Said Echatoui [1], Farid Abdi [1] and Ahmed Harrach [2]

[1] Signals, Systems and Components Laboratory (LSSC), USMBA, FST-Fez, Imouzzer road B.P 2202, Morocco

[2] Laboratory of Condensed Matter Chemistry, USMBA, FST-Fez, Imouzzer road B.P 2202, Morocco

Abstract: In this study, hydrothermal synthesis conditions for the formation of (1-x ($Na_{0.5}Bi_{0.5}$)TiO_3-x$BaTiO_3$ (x=0; 0.03; 0.05; 0.06; 0.07; 0.08 and 0.1) compounds were investigated. The process parameters such as the alkaline conditions and heating treatment (temperature, time) as well the influence of the (Na, Bi)/Ba ratio were investigated in detail. The as-prepared NBT powders were characterized by X-ray powder diffraction, scanning electron microscope (SEM) and dielectric measurements. Taking into account NBT behavior draws consideration to phenomena of the ion ordering, coexistence of various phase regions in a crystal lattice, phase transition diffusion and a considerably new phenomenon: the existence of a very high dielectric constant at low frequency. Our result presents a simple preparation route for low-cost and high-purity.

Keywords: ($Na_{0.5}Bi_{0.5}$) TiO_3; $BaTiO_3$; Hydrothermal method; Rietveld refinement; high dielectric.

Introduction

High dielectric constant materials have pulled growing attention in recent years due to their excellent potential in electromechanical actuators [1], capacitors for energy storage [2] and high-density electronic packaging technology [3]. However, the traditional dielectric materials, such as ceramics cannot gratify the rigorous exigency of advanced energy storage materials due to heat dissipation which presents a significant issue mainly in electronic devices used in a harsh environment [4, 5, 6].

To surmount these problems and to obtain a high dielectric constant in composites, several approaches have been adopted that consists of manufacturing composites based on conductive materials and polymers with ceramics. It should be mentioned that another critical issue for this materials is that the enhancement of dielectric constant is associated with dielectric loss due to the charge conduction and generation of heat in these compounds under the exposed electric field, which presents a significant disadvantage for the electronic applications [3].

In order to achieve high dielectric constant as well as low dielectric loss, the simplest way is to develop materials whose grain size is of the order of tens micrometers.

Therefore, the ability to maintain the low dielectric loss in the high dielectric ceramics over a wide composition range is a great challenge and is still an open question so far. Moreover, to the best of our knowledge, the effect of hydrothermal method and the oxide and carbonate precursor on the dielectric property is still not clear.

Moreover, the investigation of the role of morphotropic phase boundary (MPB) in determining the dielectric properties of our ceramics is necessary to have more information on BT incorporation in (1-x)($Na_{0.5}Bi_{0.5}$)TiO_3-xBa TiO_3.

Material and methods

The processes to synthesize (1-x)($Na_{0.5}$ $Bi_{0.5}$)TiO_3-x$BaTiO_3$ powders were as follows: we have used oxides (Bi_2O_3, TiO_2) of high purity, and carbonates ($BaCO_3$, Na_2CO_3) which are used as Ba and Na precursors of departure, respectively. Sodium hydroxide NaOH served as the source of sodium cations, while at the same time ensuring a strongly essential environment.

The mix was then dried and de-agglomerated using agate mortar in order to obtain the desired compositions NBT-xBT for (x=0; 0.03; 0.05; 0.06; 0.07; 0.08 and 0.1). The pH was then adjusted to 10 by dropwise addition of 10M NaOH aqueous solution. Then the mixture was transferred to a Teflon autoclave (50 ml, capacity) and kept at 180°C in a furnace for 24 h.

Finally, the precipitate which has been collected is washed several times with distilled water until the pH value of outflow reached 7 and then dried at 80 °C for 24 h.

*Corresponding author: Mohammed Mesrar
Email address: mohammed.mesrar@usmba.ac.ma
DOI: http://dx.doi.org/10.13171/mjc8319051210mm

Received February 10, 2019
Accepted March 23, 2019
Published May 12, 2019

The sintering was carried out at 1100 °C. Xpert-Pro diffractometer with CuKα (λ=1.5406Å) radiation at room temperature in the 2θ range of 10° to 80° at a scan step of 0.02°/s.

Crystallite sizes and lattice constants were determined from Rietveld refinements of the diffraction data. Raman scattering experiments were performed using a micro Raman spectrometer. Weak-field dielectric properties and dissipation factor (tan δ) in the temperature range from 40°C to 600°C and frequency region from 500Hz to 1MHz were studied using an Agilent impedance analyzer, with a rate of the temperature change was 5°C /min.

Results and Discussion

X-ray diffraction analysis

The XRD patterns of (1-x)($Na_{0.5}Bi_{0.5}$)TiO_3-xBa TiO_3 for (x=0; 0.03; 0.05; 0.06; 0.07; 0.08 and 0.1) ceramics are presented in Figure 1.

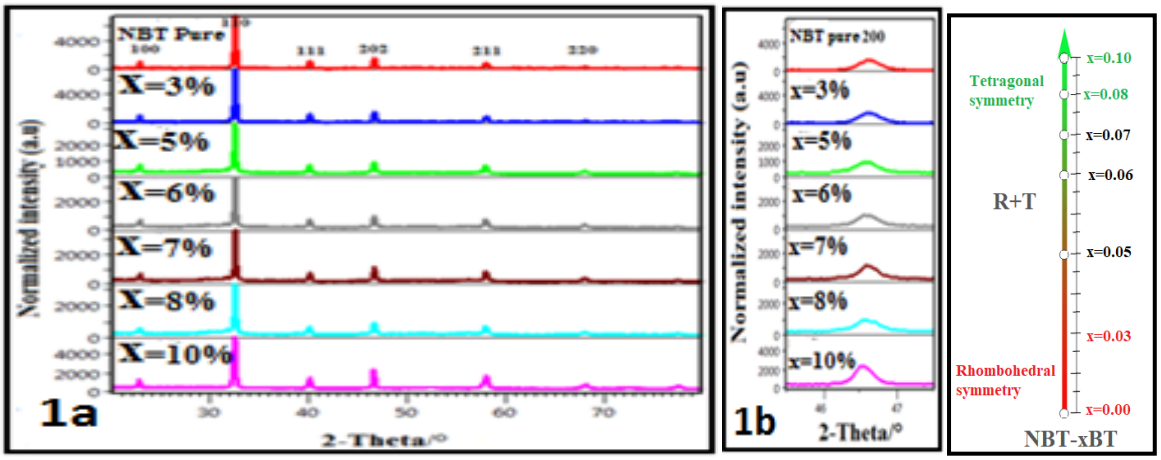

Figure 1. X-ray diffraction pattern of NBT-xBT products hydrothermally synthesized at 180°C for 24 h with NaOH concentration of 10 mol/L, with 2θ ranging a 10°–80° and b 46°–47°

The synthesized samples exhibit pure perovskite structure, and no secondary phases are detected, implying that Ba^{2+} has successfully diffused into the $Na_{0.5}Bi_{0.5}TiO_3$ lattice to form a solid solution. All peaks of the XRD pattern have been indexed with rhombohedral perovskite systems for the samples at x = 0.00 and 0.03 with space group R3c [7]. While the compositions x = 0.08 and x=0.10 have tetragonal structure with space group P4mm. As x (i.e. the concentration of $BaTiO_3$) increases, the crystal structure transforms from rhombohedral to tetragonal [7].

The XRD peaks are shifted towards the lower angle side of 2θ. This can be explained by the ionic radii of Na^+(rNa^+= 1.39 Å), and Bi^{3+}(rBi^{3+}= 1.45 Å) is smaller than that of Ba^{2+} (rBa^{2+}= 1.61 Å) inducing lattice deformation when they enter into the A-site of the host lattice [8].

Rietveld refinement analysis

Structural refinement was carried out for (1-x)($Na_{0.5}Bi_{0.5}$) TiO_3-x$BaTiO_3$ (x=0; 0.03; 0.05; 0.06; 0.07; 0.08 and 0.1) utilizing the Rietveld refinement method [9].

Rietveld refinement profiles of (1-x)($Na_{0.5}$ $Bi_{0.5}$)TiO_3-x$BaTiO_3$ were obtained employing fullprof software [10], and the fitted profiles are presented in Figure 2. The pseudo-Voigt function was used to define the peak profiles. Besides, various symmetries of spatial groups were tested by increasing compound (x) for NBT-xBT solid-solutions.

The insets of Figure 2 show the corresponding model of rhombohedral and tetragonal structures. After repeated refinement, the R_{wp} values for all the samples are all less than 8.65%. The unit-cell parameters of the as-grown NBT crystal are a=b=5.487Å, c=13.472Å and α = β =90°, γ = 120°, which are similar to the data reported in reference [11, 12].

For the x=0.05 and x=0.07 range, Rietveld refinement revealed a mixture of tetragonal (P4mm) and rhombohedral (R3c) crystalline phases. The result indicates that 0.95NBT-0.05BT is composed of 70.125% rhombohedral phase and 29.875% tetragonal phase (Table 1) these results confirmed the existence of morphotropic phase boundaries (MPB) in the NBT-xBT system.

With further refinement for range (x =0.08 and x=0.1) a tetragonal structure with space group P4mm was found to fit well. Thus, the structural phase transition from (rhombohedral +tetragonal) to tetragonal takes place with increasing BT content.

The refined profiles of (1-x)($Na_{0.5}Bi_{0.5}$)TiO_3-x$BaTiO_3$ prove the successful formation of (1-x)($Na_{0.5}Bi_{0.5}$)TiO_3-x$BaTiO_3$ phase during the heating treatment. Moreover, the characteristics of the phase structure transition were in good agreement with those reported in the literature [12, 13].

The reliability indices such as R_{wp} and R_p refined lattice parameters designate a good agreement between the refined and observed profiles with are displayed in Table 1; it also indicates the increase of the lattice parameters with the increase of BT content.

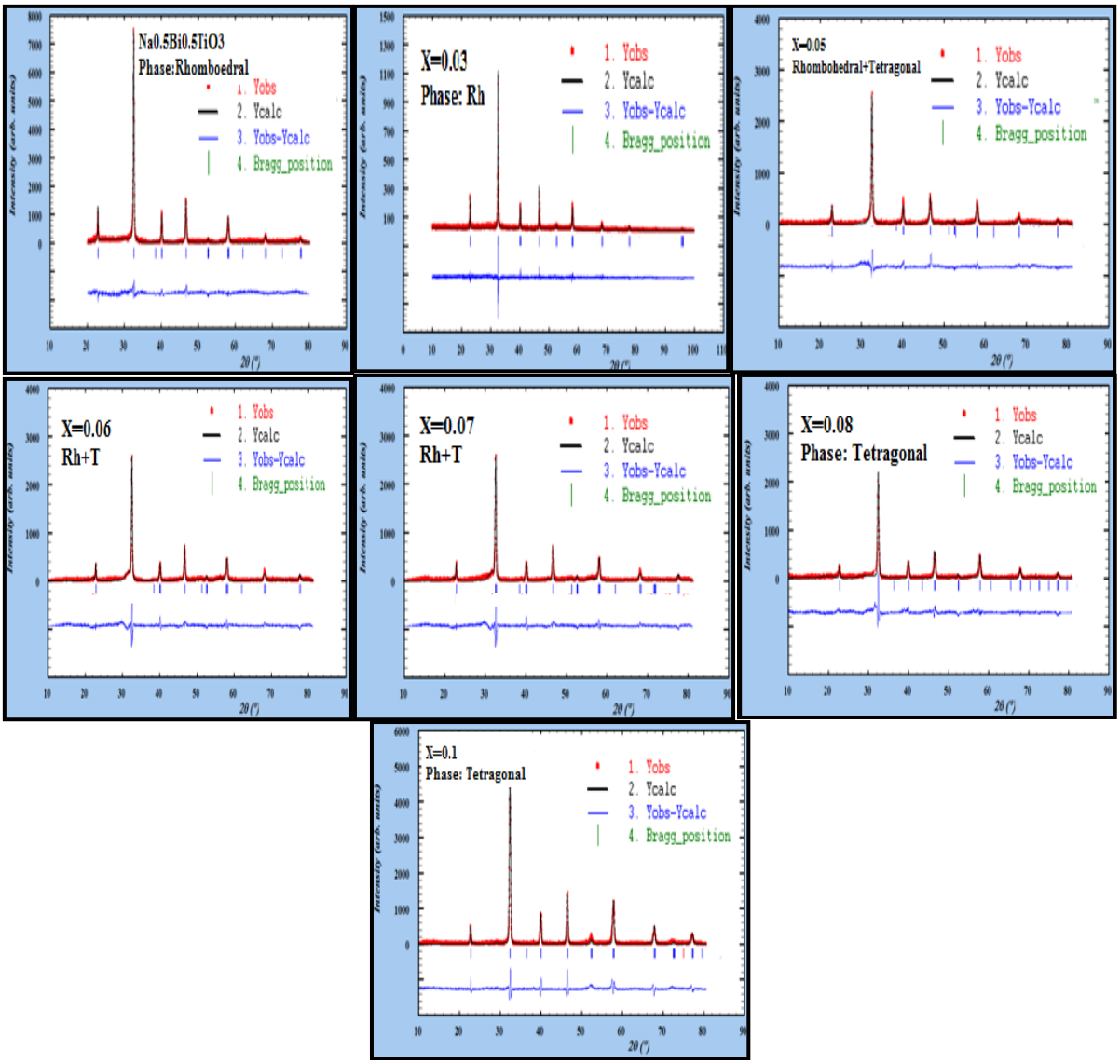

Figure 2. Rietveld Refinement for Compounds NBT-xBT

Table 1. Calculated Lattice Parameters of NBT-xBT Ceramics by Refinement

X	Phase composition	Lattice parameters			R (weighted profile)
		a (Å)	**b** (Å)	**c** (Å)	
0	R3c 100 %	5.487	5.487	13.472	8.65 %
0.03	R3c 100 %	5.494	5.494	13.482	8.63 %
0.05	R3c 70.125% P4bm 29.875 %	5.501 5.498	5.501 5.498	13.488 3.900	8.26 %
0.06	R3c 68.267% P4bm 31.733 %	5.514 5.517	5.514 5.517	13.552 3.900	8.15 %
0.07	R3c 69.763 % P4bm 30.237 %	5.519 5.515	5.519 5.515	13.554 3.901	7.32 %
0.08	P4bm 100 %	5.519	5.519	3.902	8.33 %
0.1	P4bm 100 %	5.522	5.522	3.894	8.73 %

Scanning electron microscopy analysis

The surface morphology of the synthesized samples was registered using scanning electron microscopy (SEM). The SEM images of sintered powders of all the samples are depicted in Figure 3. From the micrographs, it is found that the size and shape of the powder particles changed with $BaTiO_3$ content, while the grains show typical hexagonal geometry shape are situated in the MPB zone.

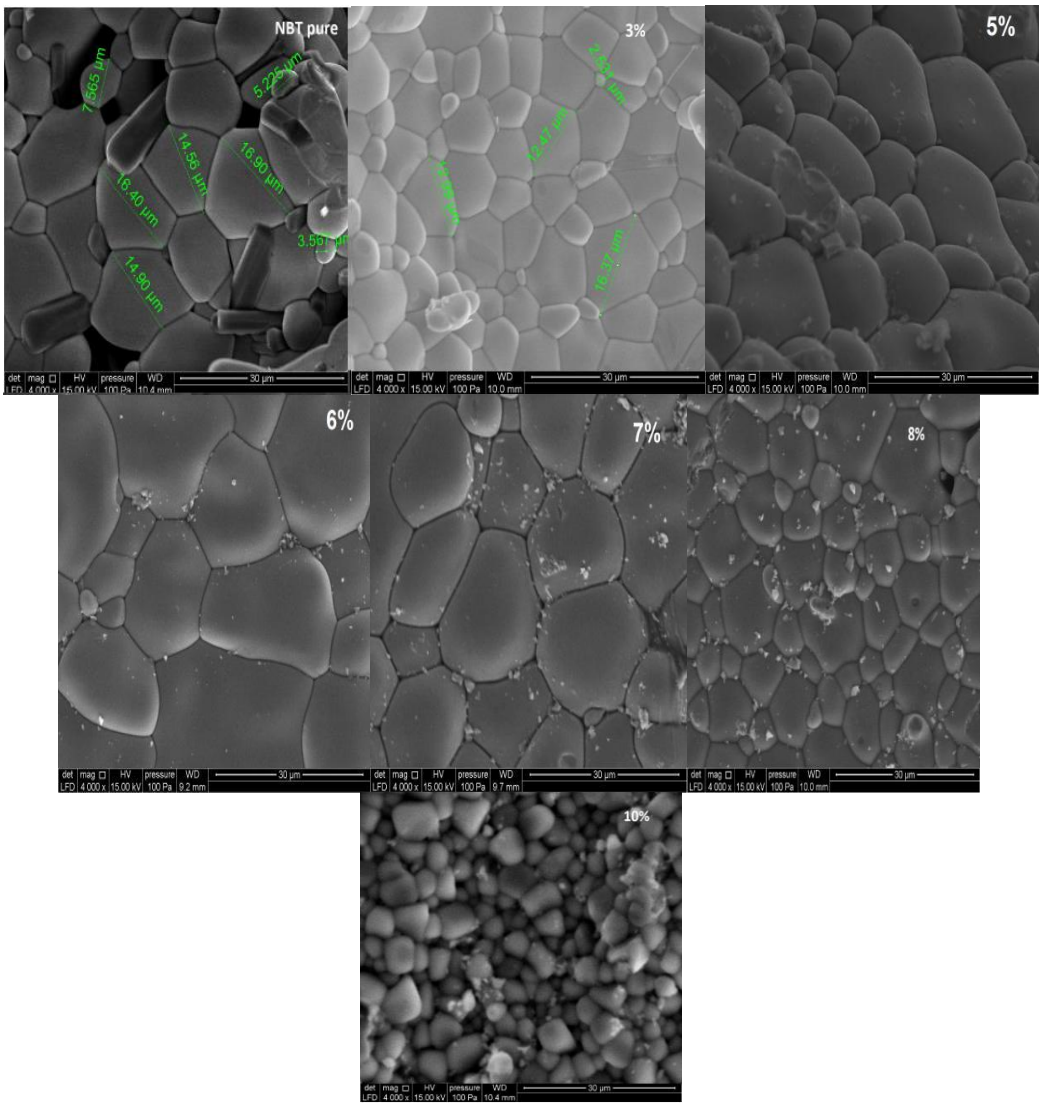

Figure 3. Cross-section SEM images of NBT-xBT ceramics

This implies that BT has diffused in NBT and it, in turn; it favours the growth of the particles. A small amount of pores is observed in the samples at (x = 0.00 and 0.1) as well as all ceramics belonging into (x =0.03; 0.05; 0.06; 0.07 and 0.08) are homogeneous and with a regular-shape with a clear grain boundary.

Experimental densities (ρex) of all the sintered NBT-xBT ceramic samples are also given in Table 2. ρex increases proportionally with the xBT content, and it becomes maximum for x=0.07, which is 6.025g/cm^3. That enhancement of density can be related to the pores disparity in the morphotropic phase boundary (MPB). However, a slight decrease of (ρex) to x = 0.1 which depends on the porosity observed.

The grains size gradually grew when the BT content is added, and it becomes max at x=0.07. Also, the value of average grain size is 24.26 µm, then decrease brutally up to 5.53 µm at x=0. 1, this reduction may also be due to the change of structure (Rh+T towards T) evoked in the XRD analysis, and confirmed by the results given in [14,15,16]. The relatively uniform grains and compact microstructure with lower porosity can be obtained at morphotropic phase boundaries (MPB).

Table 2. Micro structural parameters of the NBT-xBT ceramics.

NBT-xBT	Average grain size (µm)	Exp .density (g/cm^3)
x=0.00	11.27	5.960
x=0.03	12.47	5.990
x=0.05	20.99	6.013
x=0.06	21.88	6.019
x=0.07	24.26	6.025
x=0.08	11.81	5.920
x=0.1	5.53	5.910

Dielectric characterization

The graphs of Figure 4 present, the temperature dependences of the electric permittivity $\varepsilon_r(T)$ and dielectric losses tanδ for $(Na_{0.5}Bi_{0.5})TiO_3$. As it can be seen, $\varepsilon_r(T_m)$ and tanδ(T_m) dependences remain typical for ferroelectric materials shape and exhibit characteristic anomalies.

Two abnormal dielectric peaks can be seen in a $\varepsilon_r(T_m)$ curve, a small frequency dependent hump around 242^{0}C exhibiting the relaxor behavior indicated by T_d [15,16] (depolarization temperature) and a broad dielectric maximum, which is frequency independent about 357 ^{0}C known as T_m and this is similar to the results found by Natheer B et al. [17].

The first peak indicates the phase transition from ferroelectric to anti-ferroelectric [18,19] and the second peak represents anti-ferroelectric to a paraelectric phase transition [20, 21]. Also, the dielectric peak at T_m is frequency dispersive which implies a diffuse character for the coarse and medium-grained samples. For coarse-grained sample around in MPB, the maximum dielectric constant $\varepsilon_r(T_m)$ is 437325 at x=0.07(Table 3).
This anomaly is shifted towards higher temperatures, and the value of $\varepsilon_r(T_m)$ decreases with increase in frequency (insert in Figure 4).

After incorporation of barium ions to $(1-x)(Na_{0.5}Bi_{0.5})TiO_3$-$xBaTiO_3$ with (x= 0.05; 0.06 and 0.07) :

(i) The electric permittivity increases brutally are reaching values up to 400000 for x=0.07 (Table 3), and the main anomaly of $\varepsilon_r(T_m)$ gradually shifts towards higher temperatures, forming an inverted "U" shaped curve at low frequency.

(ii) The small anomaly of T_d connected with the anti-ferroelectric phase formation (at about 242°C for pure NBT (Figure 4) is completely disappeared for the compositions situated within MPB.

(iii) tanδ(T_m) gradually increases in the high-temperature range, and its maximum seems to shift toward higher temperatures. Moreover, for (x= 0.08 and 0.1) the $\varepsilon_r(T_m)$ curve exhibits similar behavior as pure NBT with a change in $\varepsilon_r(T_m)$ value.
These data reveal a dramatically enhanced dielectric constant for $(1-x)(Na_{0.5}Bi_{0.5})TiO_3$-$xBa\ TiO_3$ in the temperature range of 40–600 °C, yielding values over 400000, which were extremely frequency dispersive and did not affect the dielectric losses as if mentioned in Figure 4.

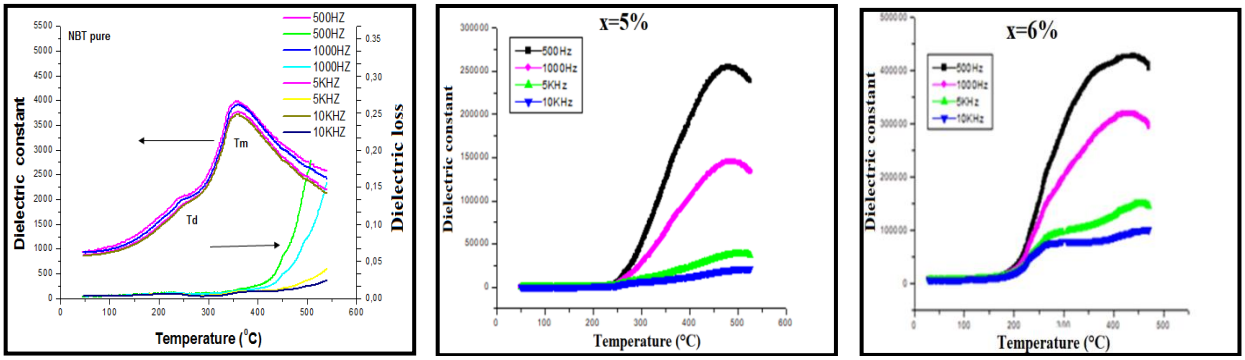

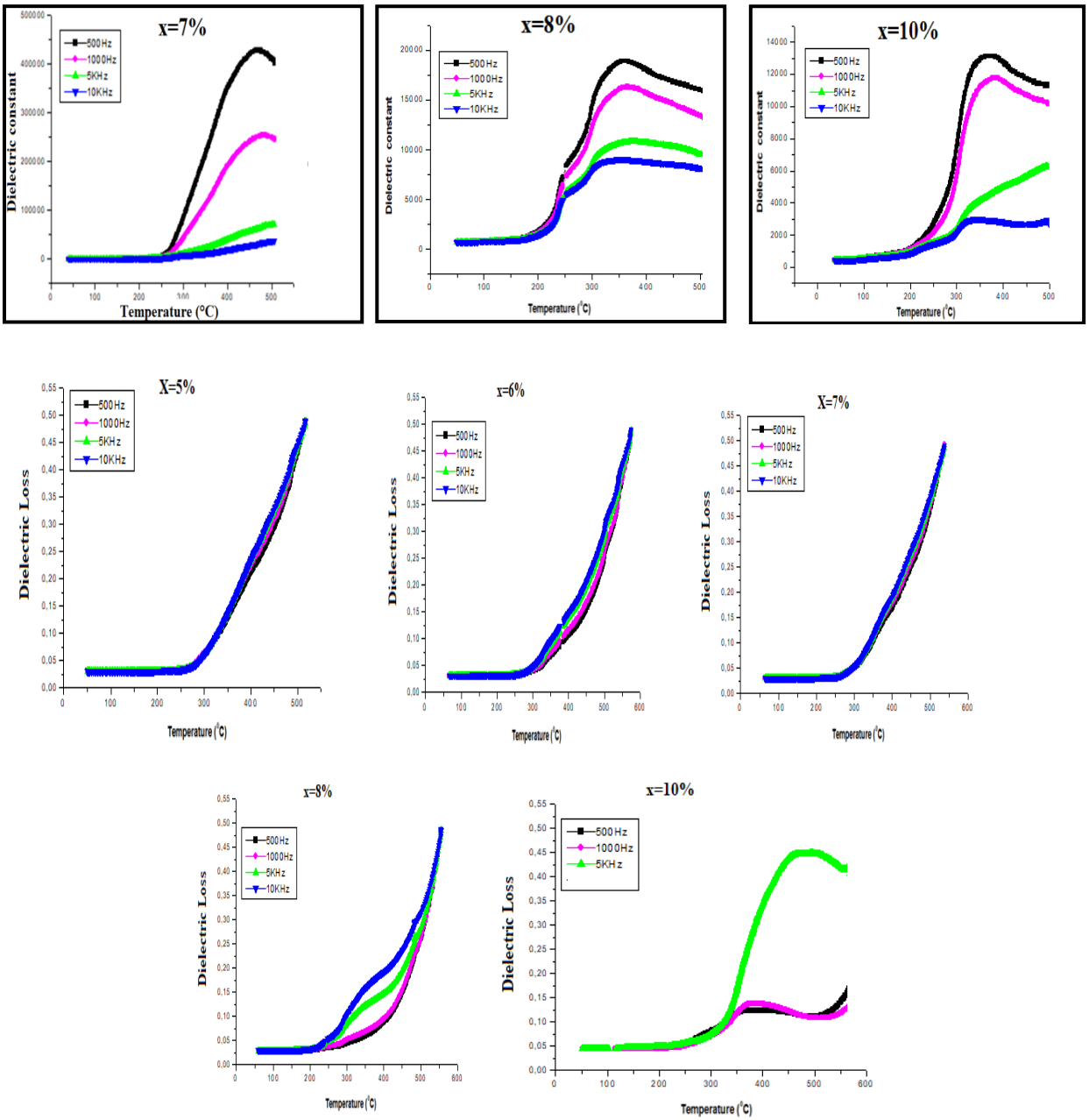

Figure. 4 Temperature dependence of the dielectric constant and loss tangent (1-x)($Na_{0.5}$ $Bi_{0.5}$)TiO_3-x$BaTiO_3$ ceramics

Table 3. Dielectric properties of NBT-xBT ceramics at 500 Hz frequency.

BT content	ε_r at Room/T°	tan δ at Room/T°	T_d (°C)	T_m (°C)	ε_r at T_m
***x*=0.00**	962	0.015	242	357	3979
***x*=0.05**	3117	0.023	-	447	49784
***x*=0.06**	3178	0.018	-	485	258338
***x*=0.07**	3247	0.024	-	468	437325
***x*=0.08**	1785	0.021	259	359	19121
***x*=0.10**	1652	0.017	242	342	13458

Conclusion

The good quality ceramics of (1-x)($Na_{0.5}$ $Bi_{0.5}$)TiO_3-x$BaTiO_3$ lead- free solid solutions were obtained by the hydrothermal method treated at a temperature of 180°C for 24 hours, we utilized, furthermore, bismuth oxide and barium carbonate as initial precursors.

X-ray diffraction study proves the formation of the crystalline structure without any trace of the secondary phase. Moreover, the Rietveld refinement method confirms the existence of MPB by the

coexistence of rhombohedral and tetragonal peaks at x=0.05-0.07. The replacement of the (Na^{+}/Bi^{3+}) ions by Ba^{2+} ions causes the increase of the mean lattice parameter of the unit cell.

The SEM images clearly show that there were no pores and no residual synthesized powder on the grains that make the microstructure is more compact with values superior of 20 µm around MPB. Moreover, the observed domain morphology shows an excellent correlation with the dielectric behavior. The dielectric constant is greatly enhanced, and low loss is obtained under dc electric field. At T_m temperature, the $\varepsilon_r(T_m)$ is increased from 3979 to 437325; the loss increased from 0.015 to 0.024 when the grain size is increased from 11.27 to 24.26 µm. It is obvious that these compounds are promising materials for low-frequency electromechanical transducer applications.

References

1- M. Rahaman, S.P. Thomas, S. Kuryan, J. Isac, K.T. Varughese, Mechanical properties of ceramic-polymer nanocomposites, Express Polym Lett., **2009**, 3, 177-189

2- Z. Liu, X. Chen, W. Peng, C. Xu, X. Dong, F. Cao, G.Wang, Temperature-dependent stability of energy storage properties of Pb0.97La0.02 (Zr0.58Sn0.335Ti0.085)O3 antiferroelectric ceramics for pulse power Capacitors, Applied Physics Letters., **2015**, 26, 262-901

3- C. Brosseau, Emerging technologies of plastic carbon nanoelectronics Surf. Coat Tech., **2011**, 206, 753-758

4- S.A. Wilson, R.P. Jourdain, Q. Zhang, R.A. Dorey, C.R. Bowen, M. Willander, C. Johansson , Mater. Sci. Eng., **2007**, 56, 1-12

5- S.M. Lukic, S. Cao, J. Bansal, R.C. Rodriguez, F. Emadi, A. Energy storage systems for automotive applications. IEEE Trans. Ind. Electron., **2008**, 55, 2258–2267

6- Y. Zhang, H. Feng, X. Wu, L. Wang, A. Zhang, T. Xia, H. Dong, X. Li, L. Zhang, L Progress of electrochemical capacitor electrode materials, International journal of hydrogen energy., **2009**, 34, 4889-4899.

7- X. Hao, A review on the dielectric materials for high energy-storage application, Journal of Advanced Dielectrics., **2013**,03,1330001

8- J. Suchanicz, T.V. Kruzina, Dielectric properties, thermal expansion and heat capacity (1-x) Na0.5Bi0.5TiO3-xBaTiO3 single crystals (x= 0, 0.02, 0.025, 0.0325 and 0.05) Mat Sci Eng B., **2013**, 178, 889-895

9- T. Takenaka, K. Maruyama, K. Sakata, (Bi, Na)TiO3-BaTiO3 system for lead-free piezoelectric ceramics, Jpn Appl Phys., **1991**, 30, 2236-2239.

10- H.M. Rietveld, A profile refinement method for nuclear and magnetic structures. Journal of Applied Crystallography., **1969**, 2, 65-71.

11- J. Rodríguez, Recent developments of the program FULLPROF, Commission on powder diffraction (IUCr)., **2001**, 26, 12-19.

12- Y. Qu, D. Shan, Effect of A-site substitution on crystal component and dielectric properties in Bi0.5Na0.5TiO3 ceramics, Materials Science and Engineering., **2005**, 121, 148-151

13- Q. Xu, Z. Song, W. Tang, H. Hao, L. Zhang, Ultra-Wide Temperature Stable Dielectrics Based on Bi0.5Na0.5TiO3–NaNbO3 System, Journal of the American Ceramic Society., **2015**, 98, 3119-3126

14- M. Mesrar, T. Lamcharfi, N. Echatoui, F. Abdi, A. Harrach, Investigation of Morphotropic Phase Boundary by Rietveld refinement and Raman Spectroscopy for (1-x)(Na0.5 Bi0.5)TiO3-xBaTiO3 Ceramics, Asian Journal of Chemistry., **2018,** 30, 1012-1018.

15- L. Liu, Z. Yang, M. Wu, L. Fang, C. Hu, Dielectric Properties of (NaBi(1-x) Kx)0.5 Ti(1-x)NbxO3 Ceramics, J. Alloys Compd., **2010,** 507, 196–200

16- C. Xu, D. Lin, K.W. Kwok, Structure Electrical Properties and Depolarization Temperature of (Bi0.5Na0.5)TiO3-BaTiO3 Lead-Free Piezoelectric Ceramics, Solid State Sci., **2008**, 10, 934-40

17- P. Vijayeta, R. K. Dwivedi, O. P. Thakur, Effect of neodymium substitution on structural and ferroelectric properties of BNT ceramics, Mater. Res. Bull., **2014**, 51,189–196.

18- N.B. Mahmood, K. Emad, Al-Shakarchi, Dielectric properties of BNT-xBT prepared by hydrothermal process, Journal of Advanced Dielectrics., **2017**, 3, 1750019

19- S.R. Kanuru, K. Baskar, R. Dhanasekaran, Synthesis, structural, morphological and electrical properties of NBT–BT ceramics for piezoelectric applications, Ceramics International., **2016**, 5, 6054-6064

20- M. Mesrar, T. Lamcharfi, N. Echatoui, F. Abdi, F.Z. Ahjyaje, Hydrothermal Synthesis of Oxide and Carbonate Powders of(1-x) (Na0.5Bi0.5) TiO3 - xBaTiO3 Ceramics, Asian Journal of Chemistry., **2019**, 31, 309-316

21- S. Pattipaka, A.R. James, P. Dobbidi, Enhanced dielectric and piezo-electric properties of BNT-KNNG piezoelectric ceramics, Journal of Alloys and Compounds, **2018**, 765, 1195-1208.